

Influence of filler and FDM printing parameters on PLA tensile strength

Anandha Moorthy Appusamy^{1), *} (ORCID ID: 0000-0001-5540-8941), Sivakumar Karuppan¹⁾ (0000-0001-7569-9037), Madheswaran Subramanian¹⁾ (0000-0001-7106-7104), Balaji Ayyanar Chinnappan²⁾ (0000-0002-2044-4683)

DOI: <https://doi.org/10.14314/polimery.2024.2.3>

Abstract: Influence of the filler (alumina, copper, carbon fiber) and FDM printing parameters on PLA tensile strength was investigated. FDM process parameters (raster angle, layer thickness, number of coatings) were optimized using the ANOVA test. It was found that the most important parameter is the raster angle. Tensile strength increases as the raster angle increases and the number of shells as well as layer thickness (larger number of infills) decreases. The highest strength was achieved for PLA/PLA-Al₂O₃.

Keywords: fused deposition modeling, 3D printing, sandwich composites, tensile strength.

Wpływ napełniacza i parametrów druku FDM na wytrzymałość na rozciąganie PLA

Streszczenie: Zbadano wpływ napełniacza (tlenek glinu, miedź, włókno węglowe) i parametrów druku FDM na wytrzymałość na rozciąganie PLA. Parametry procesu FDM (kąta rastra, grubość warstwy wewnętrznej, liczba warstw zewnętrznych) optymalizowano za pomocą testu ANOVA. Stwierdzono, że najbardziej istotnym parametrem jest kąt rastra. Wytrzymałość na rozciąganie wzrasta wraz ze wzrostem kąta rastra oraz zmniejszeniem liczby warstw zewnętrznych jak również grubości warstwy wewnętrznej (większa liczba wypełnień). Największą wytrzymałość uzyskano dla PLA/PLA-Al₂O₃.

Słowa kluczowe: druk FDM, kompozyty typu sandwich, wytrzymałość na rozciąganie.

Manufacturers in all industries are looking for light, low-cost materials with high mechanical properties for rigid 3D-printed parts production [1]. For example, the weight of the 3D-printed automobile components is developed to fulfill safety regulations without compromising the strength of the components [2–3]. In Fused Deposition Modeling (FDM) additive technology, the filament materials are melted and added layer by layer to form components of the desired shape [4]. Usage of additive technologies allows for production of geometrically complex shapes while reducing time of fabrication time, in comparison traditional manufacturing. Therefore, it is adopted in the automotive, aerospace, agriculture, fashion, medical, mechanical, and pharmaceutical industries [5–7]. In these industries, the 3D printed parts can be

used as prototype models, testing, and assembly verifications [8–9].

Additive manufacturing (AM) techniques differ on method how designed part is obtained. Based on their methodologies, AM can be divided into methods like: stereolithography (SLA), fused deposition modelling (FDM), selective laser sintering (SLS) or laminated object modelling (LOM) [10, 11].

Among the AM technologies, FDM is the most popular due to its cost effectiveness and wide range of filaments used as working materials. In the FDM process, polylactide (PLA) is one of the most used thermoplastics (approximately 240,000 tons used every year), because of its low melting point, good ability to be extruded and availability from renewable resources. Unfortunately, 3D printed PLA samples shows lower mechanical strength and elongation at break than hot-pressed samples. In this regard, the mechanical strength of the FDM-printed components is improved by optimizing the printing parameters using evolutionary algorithms, design of experiments (DOE), etc., reinforcing the filament with fillers and modifying the printer accessories. The reinforcement with different particle sizes enhances the mechanical properties such as tensile strength and Young's modulus. The reinforcement of single particles (SPS), double parti-

¹⁾ Department of Mechanical Engineering, Bannari Amman Institute of Technology, Sathyamangalam 638401, Tamilnadu, India.

²⁾ Department of Mechanical Engineering, Coimbatore Institute of Technology, Coimbatore 641014, Tamilnadu, India.

^{*} Author for correspondence:

anandhamoorthy@bitsathy.ac.in

cles (varied sizes), and triple particles (TPS), in which the double particle sizes increased the strength over the SPS and TPS due to the complete dispersion of particles in the printed part [12]. Also, the tensile strength of printed parts increases when a square-shaped nozzle is used for the FDM process. The porosity of the final 3D-printed component is reduced by 7% in comparison to the components printed using a circular-shaped nozzle. This is due to the reduced void space between the subsequent layers [12, 13]. Although modifying the printer accessories improves the tensile strength of the component, the strength can be further improved using reinforcement and optimization techniques.

The research has focused on control parameters to enhance the mechanical properties of FDM-fabricated objects [14]. Several studies attempted to optimize the FDM process parameters for improving the mechanical and electrical properties of the final printed parts [4]. The layer thickness, extrusion temperature, print speed, and raster width of a face-centered composite design (FCCD) are optimized using the Taguchi method, a fractional factorial orthogonal array (OA), and the response surface methodology technique [15]. The evaluation shows that the tensile and compressive strengths of the parts optimized through response surface methodology yield 2.81% and 8.2% higher values compared to that of the Taguchi method. The crack in the final part propagates along the printing directions due to layer orientation and plastic deformation. Hence, in addition to the raster angle and layer thickness, the build orientation is optimized using OA techniques [15–16]. In comparison to infill densities, layer thicknesses, and infill patterns, layer thickness has a significant impact on improving the mechanical strength of virgin and Re-PLA material. The strength of the final printed component is increased by using the hexagonal infill pattern [17]. This is due to the reduced void space between the layers [18]. The printed parts exhibit greater dimensional stability and strength for the smallest layer thickness. The thinnest layer reduces the void space between the layers [19].

Parts with different infill patterns, such as concentric, rectilinear, hexagon, and Herbert curve, were evaluated using different infill percentages. The results revealed that the concentric infill pattern with 100% infill demonstrates the highest tensile strength and flexural strength [20]. The change in the raster angle, increases the fill concentration of the filament, which in turn improves the mechanical strength of the final printed component [21]. It is also noted that the mechanical properties of the printed parts which were printed along the Z-axis direction is lower than the parts printed in the X-Y direction. This is because the Z-direction printed components are solely dependent on the bonding between the layers. The higher load-bearing capacity of the X-Y printed parts is due to the load sharing between the number of layers [22]. Applications that demand a higher modulus of elasticity are achieved by printing the parts in a horizontal orienta-

tion with minimal layer thickness. The storage modulus of horizontally printed parts is higher in comparison to vertically printed parts. These printed components are appropriate for high-load bearing applications [23–24]. The anisotropy property in the vertical direction of printing, influences the reduction of the ultimate and fatigue strengths of the printed parts. As a result, horizontally printed parts have greater strength than other directions [25]. The mechanical strength of the final printed part is increased by twofold when the fabrication of the parts is carried out in a high-pressure atmosphere. This is due to the improvement in the bonding between the several layers of the product. Although, the strength is increased in a high-pressure environment, the availability of such a high-pressure environment in commonly available 3D printers is not feasible [26–27]. The surface roughness of the printed parts can be minimized by minimizing the road width of the 3D-printed parts. This is because the contour of the printed parts has a minimum road width filled by a greater number of layers, which reduces the roughness [28]. The build orientation of the 3D-printed parts has a significant impact on the mechanical properties of the component. This also reduces the printing time significantly. The build orientation is combined with properties like the number of shells, infill percentage, nozzle diameter, extrusion temperature, and infill pattern [29, 30]. The machine parameters have negligible effect on the mechanical properties, but the material used to fabricate the components has a significant impact on FDM [31, 32].

The development of new materials with the necessary properties contributes to the expansion of FDM processes and applications in various industries [33]. The mechanical properties are enhanced by the reinforcement of various materials with the existing material. The composite materials for 3D printing are developed by reinforcing the base material with materials such as silicon particles, bronze, glass fiber, graphene, carbon fiber, carbon nanotubes or natural fibers like wood or bamboo. The addition of silicon particles up to 7 wt% to the PLA, increases the tensile strength of the final printed component to 95 MPa [34]. The increase in tensile strength is due to the interaction of the base materials with the reinforcement. The PLA/bronze composite increases the material's Young modulus by 33.5%, while decreasing elongation at break and yield strength by 7% [35]. Research has also been conducted to improve mechanical strength using fiber reinforcement. The chopped E-glass fiber (E-glass), thermoplastic polyurethane elastomer (TPU), and PLA-loaded composite materials outperform injection-molded composites in terms of their mechanical strength. Because of the stiffening mechanism in 3D-printed specimens, the tensile strength of the glass fiber reinforced models was reduced by 32% to 41% [36]. The homogeneous dispersion of PLA/conductive graphene (10 wt%) improves the mechanical and dynamic properties by 27% (from 31.6 MPa to 40.2 MPa) and 30% (from 1.8 GPA to

2.45 GPa), respectively [37]. The PLA/carbon black and PLA/graphene filament 3D printed structures showed no microstructural changes, but the filament resistivity was reduced 4-6 times. Due to void volume and expansion processes in thick layers, the resistivity of printed parts improved by 1500 times for printed PLA/Graphene and three hundred times for printed PLA/carbon black [38]. The compressive strength of lightweight composite materials increases when 11.5% (by volume) Kevlar fiber is added to PLA. Further, the composite printed parts strengths can be improved by increasing the density of the reinforced parts [39]. On comparing the PLA, the tensile modulus of the PLA/carbon fiber (CF) is improved 1.2-2.2 times. This is due to the fiber orientation in the printing direction, which improves stiffness along the printing path. Furthermore, the PLA/carbon fiber composite material decreases the failure strain rate due to its enhanced modulus of elasticity [40, 41].

PLA/carbon fiber reinforced thermoplastics (PLA/CFRTPC) can accommodate up to 27 wt% fiber content and increase flexural strength and modulus to 335 MPa and 30 GPa, respectively. The extrusion pressure and overlap pressure bonding, improve the flexural strength when the feed rate is increased from 60 mm/min to 80 mm/min [42]. Continuous fiber impregnation, such as CF or twisted yarn, improves the strength of printed parts. The mechanical strength and tensile modulus of carbon fiber-reinforced 3D-printed parts increased by 435 and 599%, respectively [43]. When the temperature rises from 200°C to 230°C, the continuous CF in PLA increases the bonding strength between the layers [44]. The continuous carbon fiber printed parts with different densities (20% to 100%) improve the tensile strength by 70% and the flexural strength by 18.7% [45]. Surface treatments are also used to improve the PLA and CF thermoplastics. When annealing the PLA/CF composite materials, the crystalline and ultimate strains of the PLA/CF materials are unaffected. However, the 15 wt% fiber addition enhanced the elastic modulus, by up to 78%. The voids in the printed specimens were aligned with the extrusion line, and the annealing procedure marginally reduced the voids during consolidation [46]. The agent methylene dichloride solution (8 wt%) with the PLA improves composite bonding and increases the tensile strength by 13.8% and flexural strength by 164% over unprocessed PLA/CF composites [47].

The published research is focused on printing the parts using complete mono-materials such as PLA or complete reinforced materials (composites). Authors of this work propose another way: multi-material fabrications. The sandwich parts can be fabricated using different materials; the skin and cores can be fabricated using different materials. The strength and behavior of the printed parts depend on the final parts core, shell geometry, and adhesion between the layers. Also influenced by the machine control parameters, for example, the printing direction along the loading direction increases stiffness and

Young's modulus, and edge printing increases strength and ductility [48, 49]. Various materials, such as PLA, acrylonitrile butadiene styrene (ABS), and high-impact polystyrene (HIPS), have been used in various combinations to prepare laminated parts [50]. From the investigations, researchers found that the PLA skins presented better results in tensile strength. The review investigation gives the information that sandwiching increases the properties of printed parts by using multi-material fabrication. From the review, it is observed that reinforcing materials have a large requirement for the reinforcement material compared to the base material. To overcome this, enhancing the mechanical strength through subsequent layer printing (sandwich printing) and minimal material usage is proposed in this work. However, very few studies on the fabrication of PLA sandwiches using dual-extrusion mode have been conducted. The researchers investigated mechanical properties by making the panels and core of the sandwich using the same materials; none of them investigated the sandwiches with different materials [51, 52].

This study aims to investigate the tensile properties of layered structures made of PLA/PLA-filled with aluminum oxide (Al_2O_3), carbon fiber (CF), and copper (Cu) using various FDM parameters, such as raster angles, layer thickness and number of shells.

EXPERIMENTAL PART

Materials

Poly lactide (PLA) with a density of 1.24 g/cm³ was purchased from Sun Polymers (Coimbatore, India). Aluminum oxide (Al_2O_3) particles of 150 mesh size and 99.4% purity and short carbon fiber (CF) with a diameter of 10–20 μm and a length of 100 to 200 μm were supplied by NICE Chemicals LTD (Coimbatore, India). Copper with a particle size of 35–40 μm , a mesh size of 325, and a purity of >99% was purchased from Fine Chemicals (Bengaluru, India). Wax was used as surfactant to maintain proper extrusion of the material.

Methods

The mass melt flow rate (MFR) was determined according to the ASTM D1238 standard using plastometer (Model A214, Nunes Instruments, Coimbatore, India). The measurements were carried out at a temperature of 230°C with a constant load of 3.8 kg.

Tensile properties

Tensile properties were measured using Unitek-9450 universal testing machine (UTM-FIE, India) according to ASTM-D 638 standard at room temperature at a constant crosshead speed of 5 mm/min.

Table 1. Extrusion parameters

Parameter	Value	Optimized value
Barrel temperature, °C	140–160	160
Head temperature, °C	110–130	124
Output, mm/s	100–280	165
Nozzle diameter, mm	3	–
Distance between barrel and take-off unit, m	2–4	2.4

Table 2. PLA filaments symbols and MFR data

Sample	Designation	MFR, g/10 min
PLA	M1	14.0±0.15
PLA-Al ₂ O ₃ 95/5	M2	14.8±0.10
PLA-Cu 94/6	M3	13.8±0.10
PLA-CF 92/8	M4	14.2±0.15
PLA/PLA-Al ₂ O ₃ 50/50	M5	15.1±0.10
PLA/PLA-Cu 50/50	M6	14.1±0.10
PLA/PLA-CF 50/50	M7	14.6±0.15

Morphology

After the tensile test, the fractured surface was examined using a high-capacity microscope (ICX41M, Sunny Optical Technology Co., Ltd., through Nu-Tek Solutions, India) at a magnification 100–350x.

ANOVA test

Analysis of variance (ANOVA test) was performed to determine the effect of the raster angle (0°, 45°, 90°), coating thickness (0.1, 0.2, 0.3 mm) and the number of shells (3, 4, 5) for tensile strength.

PLA filaments preparation

Reinforced PLA filaments with a diameter of 1.75 mm were obtained using a single-screw extruder with a screw diameter of 20 mm and a barrel length of 80 mm. The extrusion parameters are presented in Table 1. The composites were extruded twice to obtain uniform dispersion of the filler in the polymer matrix. Moreover, to obtain a smooth surface of the filaments and improve the fluidity of the material, a wax was used as a surfactant.

Table 2 shows designations of the obtained PLA filaments.

Samples preparation

Taguchi's L9 minimized orthogonal matrix (OA) was used to optimize the printing parameters at three levels (33: L9), as given in Table 3. The samples were printed using Flashforge Creator-3 Pro FDM 3D dual-extruder printer (Zhejiang, China) with dimensions of 227 × 148 × 150 mm. PLA and reinforced PLA were fed

Table 3. FDM control parameters

Parameter	PLA	PLA-Al ₂ O ₃	PLA-Cu	PLA-CF
Platform temperature, °C	50	50	50	50
Nozzle temperature, °C	200	235	225	240
Printing speed, mm/min	50			
Nozzle diameter, mm	0.4			
Infill pattern	Linear			
Infill density, %	100			
Raster angle, °	0, 45, 90			
Layer thickness, mm	0.1, 0.2, 0.3			
Number of shells	3, 4, 5			

through separate nozzles into the dual-extruder FDM printer.

RESULTS AND DISCUSSION

Effect of printing parameters

Table 4 illustrates the effects of the number of outer shells, raster angle and layer thickness on the tensile strength of 3D printed samples. In the case of PLA, the best results were obtained for raster angle - 90° (Level 1), layer thickness - 0.1 mm (Level 2), and number of shells - 3 (Level 3). Moreover, the raster angle has the greatest influence on tensile strength, followed by layer thickness and the number of shells. Reducing the layer thickness leads to an increase in the number of layers in the tested sample. Therefore, at the time of printing, the loads are divided by the number of layers and can withstand the load. In the case of a thicker layer, empty spaces may appear between subsequent layers, which favor the propagation of cracks. Therefore, increasing the layer thickness results in lower tensile strength.

For samples M2, M3 and M4, the tensile strength decreases with increasing layer thickness and the number of shells. Moreover, increasing the raster angle increases the tensile strength. The effect is like that of using pure PLA. Sample M5 shows better tensile strength than M1, M2, M3 and M4 at all levels. M6 also has higher strength than M1, M2, M3 and M4, but less than M5. The tensile strength of M7 is equal to that of M1 and greater than M2, M3 and M4, but lower compared to M5. It is known that reducing the layer thickness increases the number of layers in the sample, which affects the load distribution and increases the strength [5, 59]. Despite the reduction in layer thickness in CF-reinforced 3D printed parts, the tensile strength is not improved due to the presence of voids in the printed samples, as confirmed by microscopic examination (Fig. 1). The addition of PLA-CF to PLA (M7) increases tensile strength due to a stronger bond between the layers. In the case of short fibers, when

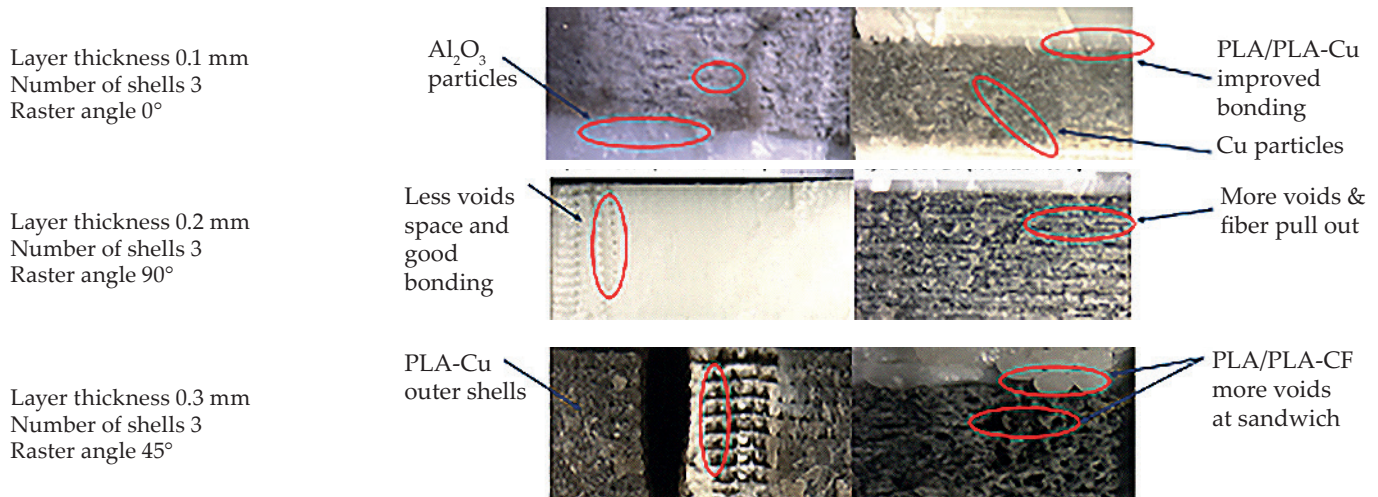


Fig. 1. View of voids in samples with selected input parameters

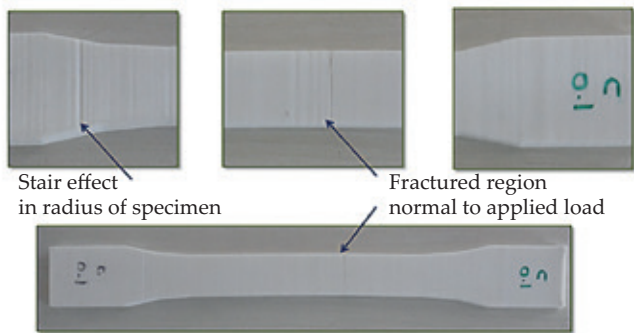


Fig. 2. Stress concentration and failure in an example printed sample

their compatibility with the polymer matrix is low, the fibers are pulled out under load (see Figure 1). This can be prevented by using continuous carbon fibers.

Premature failure of the printed sample was observed caused by stress concentration in the rounded profile (Fig. 2). due to improper infill, which initiates stress cracking.

ANOVA test analysis

To determine the parameters that have a significant impact on the tensile strength of the samples, ANOVA test was used. The statistical significance of individual parameters has been represented by the p-value. According to Taguchi *et al.*, the p-value for the 95% confidence level should be less than 0.05 [30]. The ANOVA results for tensile strength data are presented in Table 5, which shows that the p-value of the raster angle, layer thickness, and number of shells is less than 0.05 for all materials. M4 and M7 p-values for the number of shells and raster angle are greater than 0.05.

FDM extrusion of PLA-CF aligns the fibers along the deposition direction, but the ends of the short carbon fibers separate at the interface. When another layer is applied to the printed layer, the separated ends of the fiber create cavities, which causes porosity resulting in lower strength.

As a result, these printing factors have a statistically significant effect on tensile strength. The confidence interval for M1 is 96.26%, for M2 is 94.08%, for M3

Table 4. Effect of input parameters on tensile strength

Input parameters			Tensile strength, MPa						
Raster angle, °	Layer thickness mm	Shells number	M1	M2	M3	M4	M5	M6	M7
0	0.1	3	51	43	33	19	59	55	52
0	0.2	4	45	42	28	18	56	54	51
0	0.3	5	39	37	23	16	50	50	51
45	0.1	4	54	46	31	24	62	56	54
45	0.2	5	44	41	27	26	56	53	54
45	0.3	3	49	42	29	23	58	54	48
90	0.1	5	52	46	31	35	60	55	55
90	0.2	3	55	47	36	36	62	56	51
90	0.3	4	50	43	29	30	59	54	49

Table 5. Results of ANOVA test

Sample	Parameter	DF	Adj. SS	Adj. MS	f-value	p-value
M1	Regression	3	207.500	69.167	42.93	0.001
	Raster angle	1	80.667	80.667	50.07	0.001
	Layer thickness	1	60.167	60.167	37.34	0.002
	No of shells	1	66.667	66.667	41.38	0.001
	Error	5	8.1	1.6	–	–
	Total	8	215.56	–	–	–
M2	Regression	3	71.500	23.833	26.48	0.002
	Raster angle	1	32.667	32.667	36.30	0.002
	Layer thickness	1	28.167	28.167	31.30	0.003
	No of shells	1	10.667	10.667	11.85	0.018
	Error	5	4.5	0.9	–	–
	Total	8	76	–	–	–
M3	Regression	3	104.83	34.944	33.82	0.001
	Raster angle	1	24	24	23.23	0.005
	Layer thickness	1	32.667	32.667	31.61	0.002
	No of shells	1	48.167	48.167	46.61	0.001
	Error	5	5.167	1.033	–	–
	Total	8	110	–	–	–
M4	Regression	3	397.67	132.556	33.32	0.001
	Raster angle	1	384	384	96.54	0
	Layer thickness	1	13.5	13.5	3.39	0.125
	No of shells	1	0.167	0.167	0.04	0.846
	Error	5	19.889	3.978	–	–
	Total	8	417.56	–	–	–
M5	Regression	3	103.5	34.5	26.54	0.002
	Raster angle	1	42.667	42.667	32.82	0.002
	Layer thickness	1	32.667	32.667	25.13	0.004
	No of shells	1	28.167	28.167	21.67	0.006
	Error	5	6.5	1.3	–	–
	Total	8	110	–	–	–
M6	Regression	3	24.833	8.278	20.14	0.003
	Raster angle	1	6	6	14.59	0.012
	Layer thickness	1	10.667	10.667	25.95	0.004
	No of shells	1	8.167	8.167	19.86	0.007
	Error	5	2.056	0.411	–	–
	Total	8	26.889	–	–	–
M7	Regression	3	41.833	13.944	32.18	0.001
	Raster angle	1	0.167	0.167	0.38	0.562
	Layer thickness	1	28.167	28.167	65	0
	No of shells	1	13.5	13.5	31.15	0.003
	Error	5	2.167	0.433	–	–
	Total	8	44	–	–	–

is 95.03%, for M4 is 95.24%, for M5 is 94.09%, for M6 is 92.36%, and for M7 is 95.08%.

Effect of raster angle

According to Table 5, the *p*-value for the raster angle is less than 0.05, which indicates that the angle is significant at 95% confidence interval. Shells are typically applied to the inner layer to create stronger 3D printed parts. The

overlap improves adhesion between layers and reduces voids, and the stress is transferred through the outer layers of the printed element. This overlap increases as the raster angle increases from 0° to 90° and results in an increase in tensile strength (Fig. 3).

Printing the inner layers at a 90° raster angle and the shells at a 0° raster angle creates cross sandwiches that distribute stress to the outer shells, resulting in greater ductility. Stress curves for different raster angles are

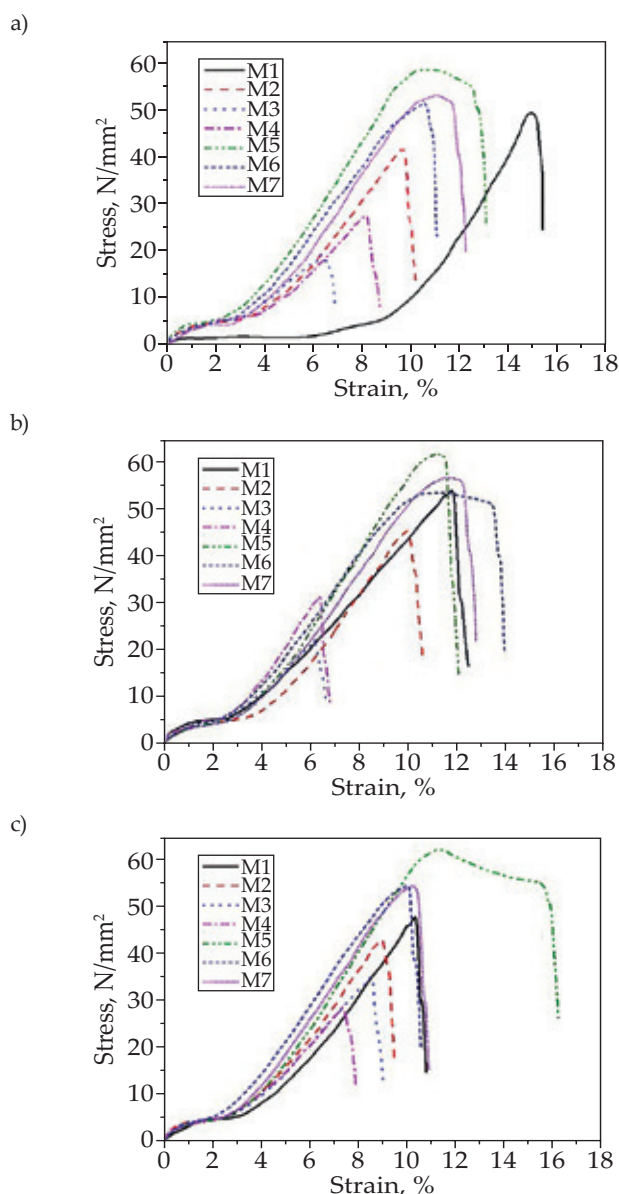


Fig. 3. Stress-strain curves at different raster angle: a) 0°, b) 45°, c) 90°

shown in Figure 3. At a raster angle of less than 45°, the layers undergo interlayer cracking and then intralayer cracking, which is also confirmed by other researchers [5, 59–61]. Parts printed at 45° and 90° angles showed better external surface and tensile strength compared to 0° angle, which is confirmed by studies of other researchers [62].

PLA shows greater elongation at 0° raster angle. The addition of filler increases the tensile strength of PLA and reduces elongation.

The maximum strength of PLA is 52 MPa at a raster angle of 90°, and the minimum is 47 MPa at an angle of 0°. Increasing the raster angle increases the layering overlap, which increases strength and reduces elongation. Tensile strength increases by 15.6% (from 27.7 to 32 MPa) for sample M4, by 15.7% (from 27.7 to 32 MPa) for sample M3, and by 4.8% (from 42 to 44 MPa) for sample M2. The

elongation decreases from 18% to 7% for an angle of 0° and from 16% to 7% for an angle of 90°. The change in the tensile behavior of the sample from ductile to brittle can be observed in the stress-strain curves (Fig. 3).

Effect of layer thickness

The p -value for layer thickness is less than 0.05 for all materials except M4 and M7 (Table 5). As a result, the layer thickness is statistically significant for the 95% confidence interval. If the layer thickness increases, the tensile strength decreases. Lower layer thickness results in more layers needed to build the part and a larger interfacial area, resulting in higher tensile strength. Due to the stronger bonding of the layers, with a smaller layer thickness, greater material stiffness is achieved, which allows it to withstand higher loads [63–64]. When CF was used, with a smaller layer thickness, greater fiber pull-out was observed at the edge of the layer than in the case of a layer with a larger thickness [14, 23]. The minimum thickness printed layer shows the more reinforced particles than the higher layer thickness printed layer.

Increasing the layer thickness reduces the tensile strength and weight of the printed parts [65]. Due to the increased layer thickness, there is less surface bonding between the layers, leading to more voids (Fig. 4), resulting in lower tensile strength. These data clearly show a correlation between the observed results and those reported by Coogan *et al.* [66] and Khunt *et al.* [67].

The maximum tensile strength was observed for a layer thickness of 0.1 mm with 3 outer shells. The addition of CF caused porosity and poor bonding, but Al₂O₃ improved bonding (Fig. 4) and increased the strength of PLA-based printed parts. In samples M4, the fibers are pulled out, and very few voids are observed in samples M3 and M2. The stress-strain curves depending on the layer thickness are shown in Figure 5. Sample M5 with a 0.1 mm layer has a maximum tensile strength of 59 MPa and an elongation of 12.5%. Increasing the layer thickness changes the mode of failure from ductile to brittle. This brittleness is caused by more voids and less bonding between the layers. At larger layer thicknesses, the crack propagates quickly between layers, causing sudden failure. The layer thickness also affects the surface quality of printed parts. The higher the layer thickness, the greater the step effects on the outer surface (greater surface roughness) [61, 68–70].

Effect of number of shells

According to Table 5, the p -value for the number of shells is less than 0.05, indicating that the number of shells is statistically significant for all materials. Tensile strength increases as the number of shells decreases (Table 4, Fig. 6). Higher values of this parameter were also observed for sandwiches. More shells reduce the required infill, reduce tensile strength by 14%, and increase the

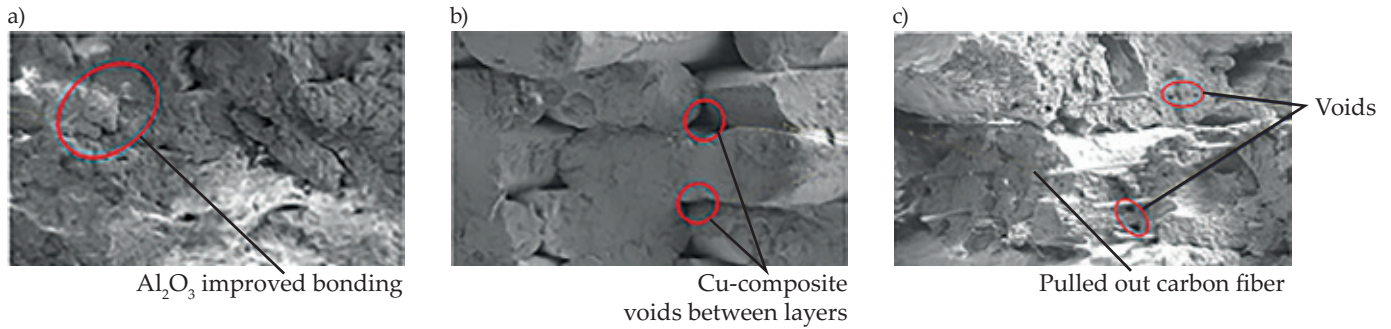


Fig. 4. Effect of layer thickness on microscopic structure. a) PLA/Al₂O₃, b) PLA/Cu, c) PLA/CF

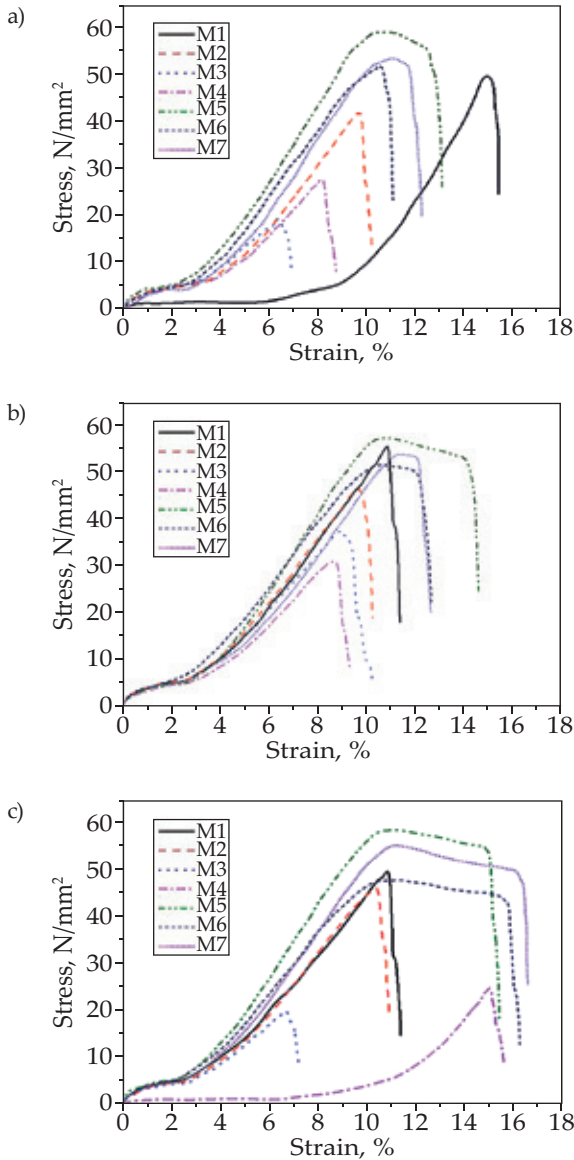


Fig. 5. Stress-strain curves at different layer thickness: a) 0.1 mm, b) 0.2 mm, c) 0.3 mm

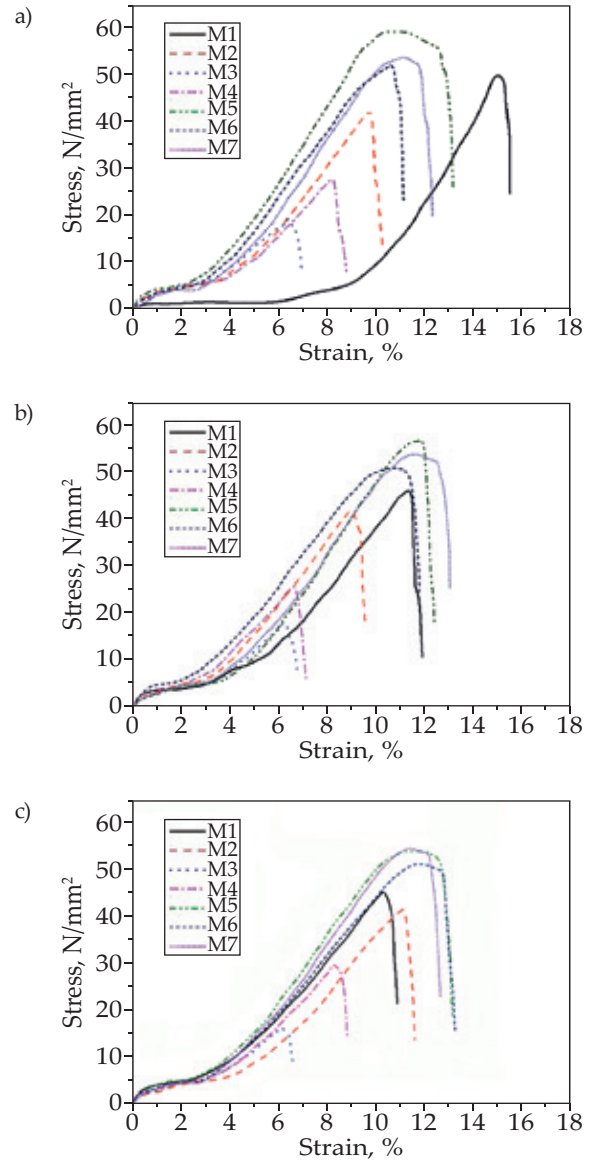


Fig. 6. Stress-strain curves varying in the numbers of shells: a) 3, b) 4, c) 5

weight of the part. This observation is consistent with the findings of other researchers [71–73].

A larger number of shells increases the empty spaces between the outer layer and the adjacent ones (Fig. 7). The voids between the layers act as a stress concentrator, which propagates cracks during loading and causes a decrease in tensile strength. When optimizing the com-

position of layer thickness, raster angle, and number of shells, it was noticed that FDM printed parts with lower layer thickness (0.1 mm), lower number of shells (3 shells), and prints above 45° angle provide good mechanical strength and surface finish. The most important parameter is the layer thickness, then the raster angle, and finally the number of shells.

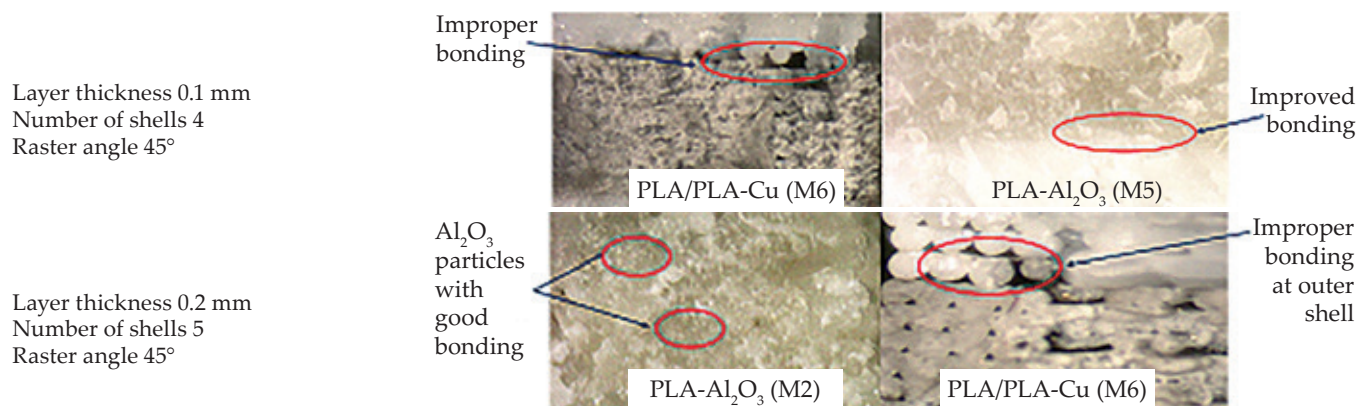


Fig. 7. Effect of the number of shells on the samples microscopic structure

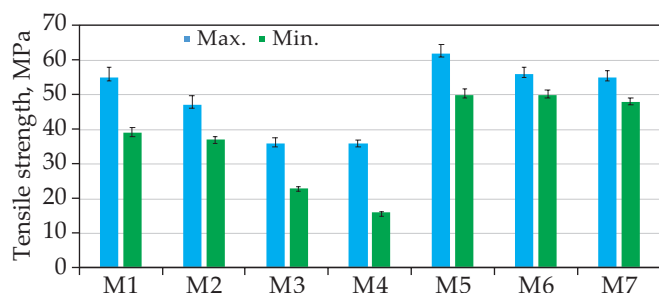


Fig. 8. Tensile strength of tested materials

Tensile strength

Fig. 8 illustrates the comparison of the tensile strengths of the tested samples. It is clearly seen that the layer-printed samples provide higher strength than the virgin samples and complete composites.

The maximum strength of M1 was shown to be higher than M2, M3 and M4, but lower than M5, M6 and M7. The minimum strength of pure PLA is greater than that of reinforced one. Moreover, the strength of the layered samples is greater than that of pure and reinforced PLA.

The improvement in the strength of layered samples is caused by increased adhesion between the contacting layers and the reduction of empty spaces between them. Overall, the layered samples had 48% greater strength compared to PETG and 80% compared to PLA-CF and PLA-Al₂O₃ [73–74].

CONCLUSIONS

PLA-based composites printed using the FDM method are characterized by limited tensile strength compared to other thermoplastic materials. To improve durability, the FDM process parameters (raster angle, layer thickness and number of coatings) should be optimized, and an appropriate modifier should be used. Therefore, Al₂O₃, copper and carbon fiber were added to PLA as reinforcement. PLA/PLA-Al₂O₃ was characterized by the highest durability. Layering improves adhesion and increases durability. Tensile strength also increases as the raster angle increases and the number of shells decreases. SEM showed that the fewer the number of shells, the fewer

voids between the layers, resulting in higher tensile strength. A smaller layer thickness (larger number of infills) increases the interfacial surface, which also results in greater tensile strength.

The sandwich 3D-printed parts can be used for applications such as car hangers that require high tensile strength and light weight. In the future, the influence of other printing parameters such as infill density, printing temperature, printing orientation, nozzle diameter, nozzle shape, extrusion speed, etc. should be investigated to determine the best set of parameters to improve the mechanical properties and other properties of 3D printed parts.

Author contribution

A.M.A. – perceived the idea, experimentation, planning, result analysis; S.K. – administration, investigation, writing-original draft, supervision; M.S. – conceptualization, methodology, investigation, formal analysis, writing-original draft; B.A.C. – developed the theoretical framework.

Funding

The authors did not receive support from any organization for the submitted work.

Conflict of interest

The authors declare no conflict of interest. All authors certify that they have no affiliations with or involvement in any organization or entity with any financial interest or non-financial interest in the subject matter or materials discussed in this manuscript.

Copyright © 2024 The publisher. Published by Łukasiewicz Research Network – Industrial Chemistry Institute. This article is an open access article distributed under the terms and conditions of the Creative Commons Attribution (CC BY-NC-ND) license (<https://creativecommons.org/licenses/by-nc-nd/4.0/>)



REFERENCES

- [1] Abdulhameed O., Al-Ahmari A., Ameen W. *et al.*: *Advances in Mechanical Engineering* **2019**, 11(2). <https://doi.org/10.1177/1687814018822880>
- [2] Romero P.E., Arribas-Barrios J., Rodriguez-Alabanda O. *et al.*: *CIRP Journal of Manufacturing Science and Technology* **2021**, 32, 396. <https://doi.org/10.1016/j.cirpj.2021.01.019>
- [3] Klippstein H., Hassanin H., Diaz De Cerio Sanchez A. *et al.*: *Advanced Engineering Materials* **2018**, 20(9), 1800290. <https://doi.org/10.1002/adem.201800290>
- [4] Durgun I., Ertan R.: *Rapid Prototyping Journal* **2014**, 20(3), 228. <https://doi.org/10.1108/RPJ-10-2012-0091>
- [5] Sood A.K., Ohdar R.K., Mahapatra S.S.: *Materials and Design* **2010**, 31(1), 287. <https://doi.org/10.1016/j.matdes.2009.06.016>
- [6] Upcraft S., Fletcher R.: *Assembly Automation* **2003**, 23(4), 318. <https://doi.org/10.1108/01445150310698634>
- [7] Chua C.K., Feng C., Lee C.W. *et al.*: *The International Journal of Advanced Manufacturing Technology* **2005**, 25, 26. <https://doi.org/10.1007/s00170-004-1865-5>
- [8] Masood S.H., Song W.Q.: *Materials and Design* **2004**, 25(7), 587. <https://doi.org/10.1016/j.matdes.2004.02.009>
- [9] Smith W.C., Dean R.W.: *Polymer Testing* **2013**, 32(8), 1306. <https://doi.org/10.1016/j.polymertesting.2013.07.014>
- [10] Kumar S., Kruth J.P.: *Materials and Design* **2010**, 31(2), 850. <https://doi.org/10.1016/j.matdes.2009.07.045>
- [11] Chua C.K., Chou S.M., Wong T.S.: *The International Journal of Advanced Manufacturing Technology* **1998**, 14, 146. <https://doi.org/10.1007/BF01322222>
- [12] Singh R., Bedi P., Fraternali F. *et al.*: *Composites Part B: Engineering* **2016**, 106, 20. <https://doi.org/10.1016/j.compositesb.2016.08.039>
- [13] Papon E.A., Haque A.: *Journal of Reinforced Plastics and Composites* **2018**, 37(6), 381. <https://doi.org/10.1177/0731684417750477>
- [14] Dey A., Yodo N.: *Journal of Manufacturing and Materials Processing* **2019**, 3(3), 64. <https://doi.org/10.3390/jmmp3030064>
- [15] Gao G., Xu F., Xu J.: *Machines* **2022**, 10(9), 750. <https://doi.org/10.3390/machines10090750>
- [16] Singh J., Goyal K.K., Kumar R. *et al.*: *Polymer Composites* **2022**, 43(9), 5908. <https://doi.org/10.1002/pc.26849>
- [17] Vinoth Babu N., Venkateshwaran N., Rajini N. *et al.*: *Materials Technology* **2022**, 37(9), 1008. <https://doi.org/10.1080/10667857.2021.1915056>
- [18] Kam M., Ipekci A., Şengül Ö.: *Journal of Thermoplastic Composite Materials* **2023**, 36(1), 307. <https://doi.org/10.1177/08927057211006459>
- [19] Torres J., Cole M., Owji A. *et al.*: *Rapid Prototyping Journal* **2016**, 22(2), 387. <https://doi.org/10.1108/RPJ-07-2014-0083>
- [20] Akhoundi B., Behravesh A.H.: *Experimental Mechanics* **2019**, 59, 883. <https://doi.org/10.1007/s11340-018-00467-y>
- [21] Hill N., Haghi M.: *Rapid Prototyping Journal* **2014**, 20(3), 221. <https://doi.org/10.1108/RPJ-04-2013-0039>
- [22] Ahn S.H., Montero M., Odell D. *et al.*: *Rapid Prototyping Journal* **2002**, 8(4), 248. <https://doi.org/10.1108/13552540210441166>
- [23] Marşavina L., Vălean C., Mărghitaş M. *et al.*: *Engineering Fracture Mechanics* **2022**, 274, 108766. <https://doi.org/10.1016/j.engfracmech.2022.108766>
- [24] Alarifi I.M.: *Polymer Composites* **2022**, 43(8), 5353. <https://doi.org/10.1002/pc.26838>
- [25] Lee J., Huang A.: *Rapid Prototyping Journal* **2013**, 19(4), 291. <https://doi.org/10.1108/13552541311323290>
- [26] Zhang Z., Long Y., Yang Z. *et al.*: *Composites Part A: Applied Science and Manufacturing* **2022**, 162, 107162. <https://doi.org/10.1016/j.compositesa.2022.107162>
- [27] Shaik Y.P., Schuster J., Katherapalli H.R. *et al.*: *Journal of Composites Science* **2022**, 6(1), 16. <https://doi.org/10.3390/jcs6010016>
- [28] Espalin D., Alberto Ramirez J., Medina F. *et al.*: *Rapid Prototyping Journal* **2014**, 20(3), 236. <https://doi.org/10.1108/RPJ-12-2012-0112>
- [29] Le L., Rabsatt M.A., Eisazadeh H. *et al.*: *International Journal of Lightweight Materials and Manufacture* **2022**, 5(2), 197. <https://doi.org/10.1016/j.ijlmm.2022.01.003>
- [30] Ahmad M.N., Ishak M.R., Mohammad Taha M. *et al.*: *Polymers* **2022**, 14(11), 2140. <https://doi.org/10.3390/polym14112140>
- [31] Mohamed O.A., Masood S.H., Bhowmik J.L. *et al.*: *Journal of Materials Engineering and Performance* **2016**, 25, 2922. <https://doi.org/10.1007/s11665-016-2157-6>
- [32] Khan S., Joshi K., Deshmukh S.: *Materials Today: Proceedings* **2022**, 50(5), 2119. <https://doi.org/10.1016/j.matpr.2021.09.433>
- [33] Roberson D., Shemelya C.M., MacDonald E. *et al.*: *Rapid Prototyping Journal* **2015**, 21(2), 137. <https://doi.org/10.1108/RPJ-12-2014-0165>
- [34] Vishal K., Rajkumar K., Sabarinathan P. *et al.*: *Silicon* **2022**, 14, 9379. <https://doi.org/10.1007/s12633-022-01712-9>
- [35] Lebedev S.M., Gefle O.S., Amitov E.T. *et al.*: *The International Journal of Advanced Manufacturing Technology* **2018**, 97, 511. <https://doi.org/10.1007/s00170-018-1953-6>
- [36] Kaynak C., Varsavas S.D.: *Journal of Thermoplastic Composite Materials* **2019**, 32(4), 501. <https://doi.org/10.1177/0892705718772867>
- [37] Prashantha K., Roger F.: *Journal of Macromolecular Science, Part A* **2017**, 54(1), 24-9. <https://doi.org/10.1080/10601325.2017.1250311>
- [38] Daniel F., Patoary N.H., Moore A.L. *et al.*: *The International Journal of Advanced Manufacturing*

- Technology* **2018**, 99, 1215.
<https://doi.org/10.1007/s00170-018-2490-z>
- [39] Hou Z., Tian X., Zhang J. *et al.*: *Composite Structures* **2018**, 184, 1005.
<https://doi.org/10.1016/j.compstruct.2017.10.080>
- [40] Ferreira R.T., Amatte I.C., Dutra T.A. *et al.*: *Composites Part B: Engineering* **2017**, 124, 88.
<https://doi.org/10.1016/j.compositesb.2017.05.013>
- [41] Hofstätter T., Pedersen D.B., Tosello G. *et al.*: *Procedia CIRP* **2017**, 66, 312.
<https://doi.org/10.1016/j.procir.2017.03.171>
- [42] Tian X., Liu T., Yang C. *et al.*: *Composites Part A: Applied Science and Manufacturing* **2016**, 88, 198.
<https://doi.org/10.1016/j.compositesa.2016.05.032>
- [43] Matsuzaki R., Ueda M., Namiki M. *et al.*: *Scientific Reports* **2016**, 6, 23058.
<https://doi.org/10.1038/srep23058>
- [44] Hofstätter T., Gutmann I.W., Koch T. *et al.*: "Distribution and Orientation of Carbon Fibers in Polylactic Acid Parts Produced by Fused Deposition Modeling", Materials from ASPE Summer Topical Meeting 2016, Raleigh, United States, June 27-30, 2016.
- [45] Yao X., Luan C., Zhang D. *et al.*: *Materials and Design* **2017**, 114, 424.
<https://doi.org/10.1016/j.matdes.2016.10.078>
- [46] Ivey M., Melenka G.W., Carey J.P. *et al.*: *Advanced Manufacturing: Polymer and Composites Science* **2017**, 3(3), 81.
<https://doi.org/10.1080/20550340.2017.1341125>
- [47] Li N., Li Y., Liu S.: *Journal of Materials Processing Technology* **2016**, 238, 218.
<https://doi.org/10.1016/j.jmatprotec.2016.07.025>
- [48] Lanzotti A., Grasso M., Staiano G. *et al.*: *Rapid Prototyping Journal* **2015**, 21(5), 604.
<https://doi.org/10.1108/RPJ-09-2014-0135>
- [49] Chacón J.M., Caminero M.A., García-Plaza E. *et al.*: *Materials and Design* **2017**, 124, 143.
<https://doi.org/10.1016/j.matdes.2017.03.065>
- [50] Baca Lopez D.M., Ahmad R.: *Polymers* **2020**, 12(3), 651.
<https://doi.org/10.3390/polym12030651>
- [51] Galatas A., Hassanin H., Zweiri Y. *et al.*: *Polymers* **2018**, 10(11), 1262.
<https://doi.org/10.3390/polym10111262>
- [52] Radadiya V.A., Gandhi A.H.: *Journal of The Institution of Engineers (India): Series C* **2022**, 103, 1049.
<https://doi.org/10.1007/s40032-022-00848-2>
- [53] Singh Boparai K., Singh R., Singh H.: *Rapid Prototyping Journal* **2016**, 22(2), 217.
<https://doi.org/10.1108/RPJ-04-2014-0052>
- [54] Yang L., Li S., Zhou X. *et al.*: *Synthetic Metals* **2019**, 253, 122.
<https://doi.org/10.1016/j.synthmet.2019.05.008>
- [55] Yang L., Li S., Li Y. *et al.*: *Journal of Materials Engineering and Performance* **2019**, 28, 169.
<https://doi.org/10.1007/s11665-018-3784-x>
- [56] Mohanty A., Nag K.S., Bagal D.K. *et al.*: *Materials Today: Proceedings* **2022**, 50(5), 893.
<https://doi.org/10.1016/j.matpr.2021.06.216>
- [57] Ferretti P., Leon-Cardenas C., Santi G.M. *et al.*: *Polymers* **2021**, 13(13), 2190.
<https://doi.org/10.3390/polym13132190>
- [58] Lee J., Lee H., Cheon K.H. *et al.*: *Additive Manufacturing* **2019**, 30, 100883.
<https://doi.org/10.1016/j.addma.2019.100883>
- [59] Uddin M.S., Sidek M.F., Faizal M.A. *et al.*: *Journal of Manufacturing Science and Engineering* **2017**, 139(8), 081018.
<https://doi.org/10.1115/1.4036713>
- [60] Bamiduro O., Owolabi G., Haile M.A. *et al.*: *Rapid Prototyping Journal* **2019**, 25(3), 462.
<https://doi.org/10.1108/RPJ-04-2018-0087>
- [61] Waseem M., Salah B., Habib T. *et al.*: *Polymers* **2020**, 12(12), 2962.
<https://doi.org/10.3390/polym12122962>
- [62] Naveed N.: *Materials Technology* **2021**, 36(5), 317.
<https://doi.org/10.1080/10667857.2020.1758475>
- [63] Son T.A., Minh P.S., Do Thanh T.: *Key Engineering Materials* **2020**, 863, 103.
<https://doi.org/10.4028/www.scientific.net/KEM.863.103>
- [64] Sheoran A.J., Kumar H.: *Materials Today: Proceedings* **2020**, 21(3), 1659.
<https://doi.org/10.1016/j.matpr.2019.11.296>
- [65] Hanon M.M., Zsidai L., Ma Q.: *Materials Today: Proceedings* **2021**, 42(5), 3089.
<https://doi.org/10.1016/j.matpr.2020.12.1246>
- [66] Coogan T.J., Kazmer D.O.: *Rapid Prototyping Journal* **2017**, 23(2), 414.
<https://doi.org/10.1108/RPJ-03-2016-0050>
- [67] Khunt C.P., Makhesana M.A., Mawandiya B.K. *et al.*: *Advances in Materials and Processing Technologies* **2022**, 8(sup2), 320.
<https://doi.org/10.1080/2374068X.2021.1927651>
- [68] Garzon-Hernandez S., Garcia-Gonzalez D., Jérusalem A. *et al.*: *Materials and Design* **2020**, 188, 108414.
<https://doi.org/10.1016/j.matdes.2019.108414>
- [69] Banerjee D., Mishra S.B., Khan M.S. *et al.*: *Materials Today: Proceedings* **2020**, 33(8), 5051.
<https://doi.org/10.1016/j.matpr.2020.02.842>
- [70] Xu Z., Fostervold R., Razavi N.: *Procedia Structural Integrity* **2021**, 33, 571.
<https://doi.org/10.1016/j.prostr.2021.10.063>
- [71] Griffiths C.A., Howarth J., De Almeida-Rowbotham G. *et al.*: *Journal of Cleaner Production* **2016**, 139, 74.
<https://doi.org/10.1016/j.jclepro.2016.07.182>
- [72] Dave H.K., Prajapati A.R., Rajpurohit S.R. *et al.*: *Advances in Materials and Processing Technologies* **2022**, 8(1), 576.
<https://doi.org/10.1080/2374068X.2020.1829951>
- [73] Bhandari S., Lopez-Anido R.A., Gardner D.J.: *Additive Manufacturing* **2019**, 30, 100922.
<https://doi.org/10.1016/j.addma.2019.100922>
- [74] Liang L., Huang T., Yu S. *et al.*: *Materials Letters* **2021**, 300, 130173.
<https://doi.org/10.1016/j.matlet.2021.130173>

Received 7 XI 2023.

Accepted 13 XII 2023.